



Hydrophilic or hydrophobic coating of whey protein aerogels obtained by supercritical-CO₂-drying: Effect on physical properties, moisture adsorption and interaction with water and oil in food systems

Lorenzo De Berardinis^a, Stella Plazzotta^{a,*}, Michele Magnan^b, Lara Manzocco^a

^a Department of Agricultural, Food, Environmental and Animal Sciences, University of Udine, Via Sondrio 2/A, 33100 Udine, Italy

^b Polytechnic Department of Engineering and Architecture, University of Udine, Via delle Scienze 208, 33100 Udine, Italy

ARTICLE INFO

Keywords:

Porous ingredients
Alginate
Agar
Ethylcellulose
Water and oil uptake

ABSTRACT

Aerogel monoliths, prepared by water-to-ethanol substitution and supercritical-CO₂-drying of whey protein hydrogels, were dip-coated with hydrophilic (alginate, AL; agar, AG) or hydrophobic (ethylcellulose, EC) polymers. AL coating induced aerogel collapse, due to solvent absorption. AG and EC rapidly set onto aerogel surface, forming layers of 65 and 100 μm thickness, respectively. While AG-coating induced 20% volume shrinkage, 25% apparent density increase and 75% firmness increase, EC-coating maintained the original aerogel structure. Upon exposure to 100% equilibrium relative humidity, aerogels showed moisture uptake in the order AG-coated > uncoated > EC-coated. When immersed in water or oil, the AG-coated aerogel showed an uptake respectively 40 and 60% lower than the uncoated control. The oil barrier capacity of AG-coated aerogel was also demonstrated in a lipid food system (stearin-oil mixture). Although not reducing oil uptake, EC-coating reduced water uptake by 30% and its water barrier properties were demonstrated upon immersion in an aqueous food system (water-flour batter).

Industrial relevance: The obtained results indicate tailored coating as a feasible strategy to enhance aerogel functionality in food. This would open further possibilities, including the use of aerogels as smart food ingredients able to modulate aroma and bioactive delivery both in the food product and during digestion. These findings are thus important in supporting the industrial development of aerogel-based ingredients with customized functionalities.

1. Introduction

Aerogels are nanostructured porous materials characterized by low density (0.0003–0.5 g/cm³) and high porosity (70.0–99.8%) (Fricke & Tillotson, 1997). Aerogels could be developed starting from inorganic or organic compounds. Thanks to their biodegradability and biocompatibility, carbohydrates and/or proteins have been demonstrated to be ideal precursors for the development of bio-based aerogels, also called bioaerogels, to be applied in different life-science fields, including environmental, pharmaceutical, and biomedical sectors (García-González et al., 2015; Plazzotta et al., 2020). More recently, aerogels have attracted great attention in the food sector, where their unique properties could be exploited to develop ingredients with novel properties and functionalities (Jung et al., 2023; Manzocco et al., 2021; Plazzotta et al., 2021).

Bioaerogels are obtained by removing water from a hydrogel of the selected biopolymer, with a proper technique able to preserve the original gel structure (García-González & Smirnova, 2013). If air-drying is applied, the capillary tensions associated with liquid-vapour interfaces lead to extensive network collapse. Alternatively, water gel can be removed by sublimation, by exploiting freeze-drying. This technique is however usually associated with a ballooning effect of growing ice crystals, which causes network cracking (Ciuffarin et al., 2023). For these reasons, the golden standard for aerogel production is represented by supercritical-CO₂ drying. In this case, gel water is preliminarily substituted with ethanol which is then removed by a flow of CO₂ in the supercritical state. The high solubility of ethanol in dense phase CO₂ and the peculiar solvating and permeating properties of the latter guarantee the minimization of capillary forces during solvent removal, avoiding structural collapse, thus leading to highly porous bioaerogels (García-

* Corresponding author.

E-mail address: stella.plazzotta@uniud.it (S. Plazzotta).

<https://doi.org/10.1016/j.ifsset.2023.103530>

Received 4 June 2023; Received in revised form 10 October 2023; Accepted 28 November 2023

Available online 1 December 2023

1466-8564/© 2023 The Authors. Published by Elsevier Ltd. This is an open access article under the CC BY license (<http://creativecommons.org/licenses/by/4.0/>).

González et al., 2019).

The essential characteristic of aerogels is their open porosity, made by pores connected and accessible from the surface (Naftaly et al., 2020). The open porosity of aerogels is at the basis of their capacity to load bioactive or flavour compounds, making these materials optimal candidates as delivery systems in foods. For instance, up to 0.2 g/g_{aerogel} of resveratrol was loaded into alginate aerogels (dos Santos et al., 2020). A similar loading potential was reported for tocopherol and phytosterol loaded into starch aerogel (De Marco & Reverchon, 2017; Ubeyitogullari et al., 2019). Because of their high internal pore volume, aerogels can also accommodate huge amounts of different liquids, including water, solutions of salts and polar molecules, surfactants, and oils. In this regard, whey protein and alginate aerogels were shown to absorb about 5 and 80 g_{water}/g_{aerogel}, respectively (Mallepally et al., 2013; Manzocco et al., 2022), while κ-carrageenan and whey protein aerogels have been loaded with 4.3 and 5.6 g/g_{aerogel} of sunflower oil, respectively (Manzocco et al., 2017; Plazzotta et al., 2020).

Besides the loading potential, even the unloaded skeleton of aerogels could have interesting food-related functionalities. Indeed, the use of porous aerogels could represent an interesting strategy to reduce the calorie density of food products, by partially replacing their volume with air (Osterholt et al., 2007). Aerogel-mediated air incorporation could also be used to steer food sensory perception. The presence of air within a porous structure entrapping sugar or salt has been associated with an increase in sweetness and saltiness perception, potentially allowing the reduction of sugar or salt added to food (Chiu et al., 2015).

While the open porosity of aerogels is an essential feature driving their functionality, it might also represent a critical issue when it comes to aerogel application as food ingredients. Open porosity make aerogels highly prone to moisture adsorption, which might cause their structural collapse. It has been demonstrated that whey protein aerogels evolved from a glassy to a rubbery state when stored at equilibrium relative humidity (ERH) higher than ~80% for 48 h, losing the original porosity (Manzocco et al., 2022). Similarly, κ-carrageenan aerogels collapsed when maintained at ERH higher than 60% (Manzocco et al., 2017). Structural collapse may occur even faster when the aerogels are placed in contact with water during food formulation. Whey protein, egg white protein and sodium caseinate aerogels significantly swelled upon contact with water and aqueous solutions (Kleemann et al., 2020; Manzocco et al., 2022). In the case of κ-carrageenan aerogels immersed in water, complete solubilization was observed (Manzocco et al., 2017). Further interaction with aqueous environments inevitably occurs when the aerogels are ingested and come into contact with the digestive fluids. In this regard, it was demonstrated that aerogel swelling during digestion can modify the release of loaded molecules (Kleemann et al., 2020; Plazzotta et al., 2022).

Preserving the inner porous structure of aerogels is thus pivotal to optimize their functionality as food ingredients. The application of an external protective layer on the surface of aerogels could represent a promising strategy. However, only limited information is reported on the possibility of coating bioaerogels with food-grade materials. Goslinska et al. (2019) showed that whey protein aerogels can be covered with an alcoholic solution of shellac, which directly crystallises on the surface of the aerogel upon solvent evaporation. In addition, Schroeter et al. (2021) demonstrated the potentiality to control the release of vanillin from cellulose aerogel particles in water by acting on the thicknesses of the shellac-coating layer. The use of hydrophobic shellac coating could help control the structure of the aerogel when used as an ingredient of water-containing foods. Nevertheless, food systems not only contain water as the main solvent but might also include a relevant amount of lipid components such as oils. The latter may also modify aerogel physical properties, as demonstrated for whey protein aerogels, which undergo volume contraction upon oil absorption (Manzocco et al., 2022).

Based on these considerations, the present work aims at widening the functionality of whey protein aerogels as food ingredients by coating

them with both hydrophilic (i.e., alginate and agar) and lipophilic (i.e., ethylcellulose) surface layers. To this aim, whey protein aerogels were dipped into aqueous solutions of alginate or agar, or in an ethanol solution of ethylcellulose. The solvent was then removed by evaporation to allow the formation of the coating layer. Coated aerogels were analyzed for structural properties (microstructure, volume shrinkage, firmness), ability to adsorb environmental moisture and capacity of solvent absorption from food systems with increasing complexity (water, oil, flour-water dough, coconut stearin-oil mixture). The effect of coating application was assessed by comparison of the structural and functional properties of the coated aerogels with those of the uncoated ones. The efficacy of coating in preserving aerogel structure when inserted in food was thus demonstrated for the first time.

2. Materials and methods

2.1. Materials

Whey protein isolate (WP, 94.7% protein content; 74.6% β-lactoglobulin, 23.8% α-lactalbumin, 1.6% bovine serum albumin) was purchased from Davisco Food International Inc. (Le Sueur, MN, USA) Sigma-Aldrich (Milan, Italy); hydrochloric acid (HCl) and absolute ethanol (purity ≥99.8%) were purchased from Carlo Erba Reagents (Milan, Italy); liquid carbon dioxide (CO₂) (purity 99.995%) was purchased from Sapio (Monza, Italy); phosphorus pentoxide (P₂O₅) was purchased from Chem-Lab NV (Zedelgem, Belgium); alginate (AL), calcium carbonate and glycerol were purchased from Sigma-Aldrich (St. Louis, United States); agar (AG, Agar Technical) was purchased from Thermo Fisher Scientific (Waltham, United States); ethylcellulose (EC, ETHOCEL™ Standard 100 FP Premium) was purchased from Dow Chemical (Midland, United States); “00” flour (pastry flour) and sunflower oil were purchased in a local market; coconut stearin was kindly provided by an Italian company engaged in the production of fats and oils. Bidistilled water, purified with System advantage A10® (Millipore S.A.S, Molsheim, France) was used.

2.2. Preparation of whey protein aerogels

WP aerogels were prepared as described by Manzocco et al. (2022). Briefly, 20% (w/w) WP was suspended in water and allowed to completely rehydrate by stirring 2 h at room temperature and overnight at 4 °C. The protein suspension was adjusted at pH 4.8 (pH-Meter BASIC 20, Crison, Barcelona, Spain) with 1 M HCl. Aliquots of 50 mL of the protein suspension were introduced in Falcon tubes and thermally gelled in a water bath (90 °C, 20 min), cooled in an ice bath for 15 min, and stored in a refrigerated cell (4 ± 2 °C) for 24 h. The WP hydrogel was removed from the tubes and cut into cylinders with a height of 2.0 ± 0.1 cm and a diameter of 2.5 ± 0.1 cm. Hydrogel cylinders were then converted into aerogel monoliths as previously described by Manzocco et al. (2017). In particular, hydrogel cylinders were subjected to progressive water substitution with food-grade ethanol and dried in a supercritical-CO₂ plant, by a flow of CO₂ at 11 ± 1 MPa and 45 °C. The obtained WP aerogel monoliths were stored in desiccators containing P₂O₅ at room temperature until use.

2.3. Preparation of alginate coating solution

AL coating solution was obtained according to Fernandes et al. (2018), with some modifications. AL powder (3%, w/w) was dissolved in water at 60 °C for 1 h under stirring. Subsequently, 1% (w/w) glycerol was added to the AL solution, followed by a further 10 min stirring at 60 °C. Then, 1% (w/w) calcium carbonate was added and the solution was further stirred for 30 min at 60 °C. The solution was cooled down to 37 °C and kept at this temperature under stirring until use.

2.4. Preparation of agar coating solution

AG coating solution was prepared according to Arham et al. (2016), with minor modifications. AG powder (3%, w/w) was dissolved in water at 90 °C for 30 min under gentle stirring. Subsequently, 10% (w/w) glycerol was added, followed by a further 10 min stirring at 90 °C. The solution was cooled down to 37 °C and maintained at this temperature under stirring until use.

2.5. Preparation of ethylcellulose coating solution

EC coating solution was obtained as previously described by Hjartstam and Hjertberg (1999), with some adjustments. EC was dissolved in absolute ethanol (10% w/w) at 90 °C for 30 min under stirring until use.

2.6. Aerogel coating

In the case of AL and AG coating, aerogel monoliths, held by metal clips, were dipped for 3 s in the coating solution. Metal clips, holding the dipped monoliths, were suspended on a hanging rack at -20 °C for 2 min. Upon monolith removal from the metal clips, one droplet of the coating solution was added onto the surface originally covered by the clips during dipping. Monoliths were further placed at -20 °C for 2 min and stored at 4 °C for 8 h to allow coating setting. Samples were then dried in a forced-air drier (30% FAN, 50% FLAP) (DETAILS) for 24 h at 37 °C. This temperature was selected since below the ones associated with the gel-sol transition of AG (~ 40 °C).

EC coating was performed using the same methodology applied for AL and AG coating with the following modifications: monolith dipped in the EC ethanolic solution was suspended on the hanging rack at room temperature under a laboratory hood for 1 h, before and after clip removal, to allow both coating setting and ethanol evaporation.

Coated WP aerogels were stored in desiccators containing P₂O₅ at room temperature until use.

2.7. Volume and apparent density

Aerogel volume was determined by measuring the diameter and height with CD-15APXR digital calibre (Absolute AOS Digimatic, Mitutoyo Corporation, Kanagawa, Japan). Volume changes were expressed as the percentage ratio between the sample volume and the volume of the corresponding uncoated aerogel. Apparent density was calculated as the ratio of the aerogel weight and volume and expressed as g cm⁻³.

2.8. Porosity and pore volume

Apparent density (ρ_a , g cm⁻³, paragraph 2.7) and whey protein skeletal density ($\rho_s = 1.35$ g cm⁻³, Fischer et al., 2004) were used to calculate aerogel porosity (Eq. (1)) and pore volume (Eq. (2)):

$$\text{Porosity (\%)} = 1 - \frac{\rho_a}{\rho_s} \bullet 100 \quad (1)$$

$$\text{Pore volume (cm}^3\text{ g}^{-1}\text{)} = \frac{1}{\rho_a} - \frac{1}{\rho_s} \quad (2)$$

2.9. Firmness

Firmness was determined by uniaxial compression test using an Instron 4301 (Instron LTD., High Wycombe, UK). Samples were tested with a 6.2 mm diameter cylindrical probe fixed on a 1000 N compression head at 25 mm/min crosshead speed. Force-distance curves were obtained from the compression test and firmness was expressed as the maximum force (N) required to penetrate the sample for 2 mm.

2.10. Image acquisition

An image acquisition cabinet (Immagini & Computer, Bareggio, Italy) set with a digital camera (EOS 550D, Canon, Milano, Italy) was used. The camera was positioned on an adjustable stand positioned 50 cm above a black cardboard base where the samples were positioned. The light was provided by 4 × 100 W frosted photographic floodlights, set to minimize shadow and glare.

2.11. Scanning electron microscope analysis (SEM)

Samples were mounted on aluminium holders and sputter-coated with 10 nm of gold using a Sputter Coater 108 auto (Cressington Scientific Instruments, Watford, United Kingdom). The samples were then observed in a SEM unit (EVO 40XVP, Carl Zeiss, Milan, Italy), at ambient temperature and under vacuum. Samples images were taken using an acceleration voltage of 20 kV and the SmartSEM v. 5.09 application software (Carl Zeiss, Milan, Italy) was used to acquire the images of the samples at magnification from 100× to 25,000 × .

2.12. Moisture adsorption

Samples were weighed, transferred into weighing bottles and placed in desiccators containing water at room temperature (22 °C) until a constant weight in three consecutive measurements was achieved. Adsorbed water vapour was expressed as the ratio of weight gain at time *t* (min) and the initial volume of the aerogel. Data were expressed as g water vapour per cm³ aerogel.

2.13. Preparation of model systems

The aqueous model system was prepared by manually mixing flour with 61% (w/w) water until obtaining a homogeneous batter. The lipidic model system was obtained by manually mixing coconut stearin with 34% (w/w) sunflower oil. The lipidic mixture was heated under stirring at 50 °C for 30 min, and cooled at room temperature (22 °C).

2.14. Water and oil uptake

Samples were immersed into 250 mL beakers containing 125 mL of water, sunflower oil, aqueous or lipidic model system at room temperature (22 °C). At defined times, samples were removed from the beaker, carefully drained with absorbent paper to remove the not-absorbed solvent and weighed till a constant weight in three consecutive measurements was achieved. Absorbed solvent was expressed as the ratio of weight gain at time *t* (min) and the initial volume of the aerogel. Data were expressed as g solvent per cm³ aerogel.

2.15. Data analysis

Determinations were expressed as the mean ± standard error of at least three repeated measurements from two experiment replicates. Statistical analysis was performed by using R ver. 4.2.2 (The R Foundation for Statistical Computing). A one-way analysis of variance (ANOVA) was carried out. Significantly different samples were determined using the Tukey test (*p* < 0.05). Non-linear regression analysis was performed by using TableCurve2D software (Jandel Scientific, ver. 5.01). The goodness of fit was evaluated based on statistical parameters of fitting (R²).


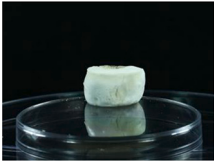
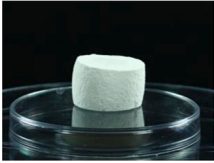
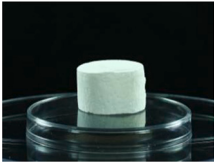
3. Results and discussion

3.1. Structural characterization of coated aerogels

Table 1 reports the appearance of whey protein (WP) aerogels before and after dip coating with hydrophilic polymers, namely alginate (AL)

Table 1

Appearance, volume, apparent density and firmness of aerogels coated with alginate, agar or ethylcellulose. Uncoated aerogel is also shown as control.

Coating	Appearance	Volume (cm ³)	Apparent density (g cm ⁻³)	Porosity (%)	Pore volume (cm ³ g ⁻¹)	Firmness (N)
Uncoated		5.82 ± 0.23 ^a	0.28 ± 0.01 ^b	79.1 ± 0.8 ^a	2.8 ± 0.1 ^a	51.50 ± 2.47 ^c
Alginate		ND*	ND*	ND*	ND*	ND*
Agar		4.64 ± 0.30 ^b	0.35 ± 0.02 ^a	74.1 ± 1.9 ^b	2.1 ± 0.2 ^b	89.59 ± 3.77 ^a
Ethylcellulose		5.85 ± 0.10 ^a	0.28 ± 0.01 ^b	79.3 ± 0.4 ^a	2.8 ± 0.1 ^a	60.03 ± 4.73 ^b

^a, ^b, ^c: means indicated by different letters in the same column are significantly different ($p < 0.05$).

* ND: not determined due to aerogel structural collapse.

and agar (AG), or hydrophobic ethylcellulose (EC). The uncoated aerogel presented the typical white appearance resulting from intense light scattering of highly porous WP aerogels (Betz et al., 2012; Manzocco et al., 2022). In this regard, the porous structure of the control sample was demonstrated by the assessment of porosity and pore volume. The results reported in Table 1 show values around 80% and 2.8 cm³ g⁻¹, respectively, which are in line with those reported in the literature for protein aerogels (Betz et al., 2012; Selmer et al., 2015). Aerogels coated with AL and EC appeared similarly white, due to the transparency of the used coatings (Kim et al., 2020; Parreidt et al., 2018). By contrast, the AG-coated sample appeared yellowish, due to the colour of AG. Coating with AL led to a significant volume shrinkage, with evident loss of the original shape. The latter was observed immediately after dipping in the alginate aqueous solution (data not shown), suggesting that structural collapse was due to extensive absorption of water from the coating solution into the aerogel pores (Alnaief et al., 2012). By contrast, in the case of the AG coating, no evident modification of the aerogel shape was observed just after dipping in the aqueous solution (data not shown). Volume shrinkage and consequent increase in aerogel apparent density were detected during the following 24 h-drying (Table 1). These changes were attributed to the slow migration of water from the surface AG gel into the aerogel pores during drying. This water migration caused significant volume shrinkage and aerogel stiffening, due to the reduction of the void fraction inside the aerogel structure. The latter was demonstrated by porosity and pore volume data, which were statistically lower than those of the control sample (Table 1). Although these structural modifications, the density and porosity values obtained for the AG-

coated sample aligned with those typically reported for aerogels (Fricke & Tillotson, 1997). On the opposite, no volume change was observed in the case of the EC-coated sample, which also showed porosity and pore volume values comparable to those of the control aerogel (Table 1). This suggests that EC-coating did not affect the original porous structure of the aerogel. Such results are probably due to the different nature of the solvent of the dipping solution (Romero-Bastida et al., 2004; Sousa et al., 2010): while AG and AL were solubilized in water, an alcoholic EC dipping solution was used. Upon aerogel dipping into the alcoholic EC solution, ethanol quickly evaporated from the EC gel layer, leading to a dried EC coating layer within 2 h at room temperature. Despite no significant changes in aerogel volume were detected, the EC-coated aerogel presented a higher firmness as compared to the uncoated one (Table 1), suggesting that mechanisms other than aerogel structural collapse could be involved. To further study the structural effect of coating on the aerogels, SEM images were captured both at the aerogel surface and at the aerogel/coating contact point (Fig. 1).

The surface and section of the uncoated aerogel (Fig. 1) were characterized by the presence of dried spherical aggregates (microgels) interlinked in a continuous network with fine porosity. By comparison with the scale bar, pores with dimensions in the range 1–5 μm were identified. Such structure is in line with previously reported data on WP aerogels obtained at the isoelectric point (Manzocco et al., 2022; Plaz-zotta et al., 2021). The application of AL coating led to the complete collapse of the aerogel structure, with no evidence of the original WP microgel architecture (Fig. 1). This result is in agreement with the

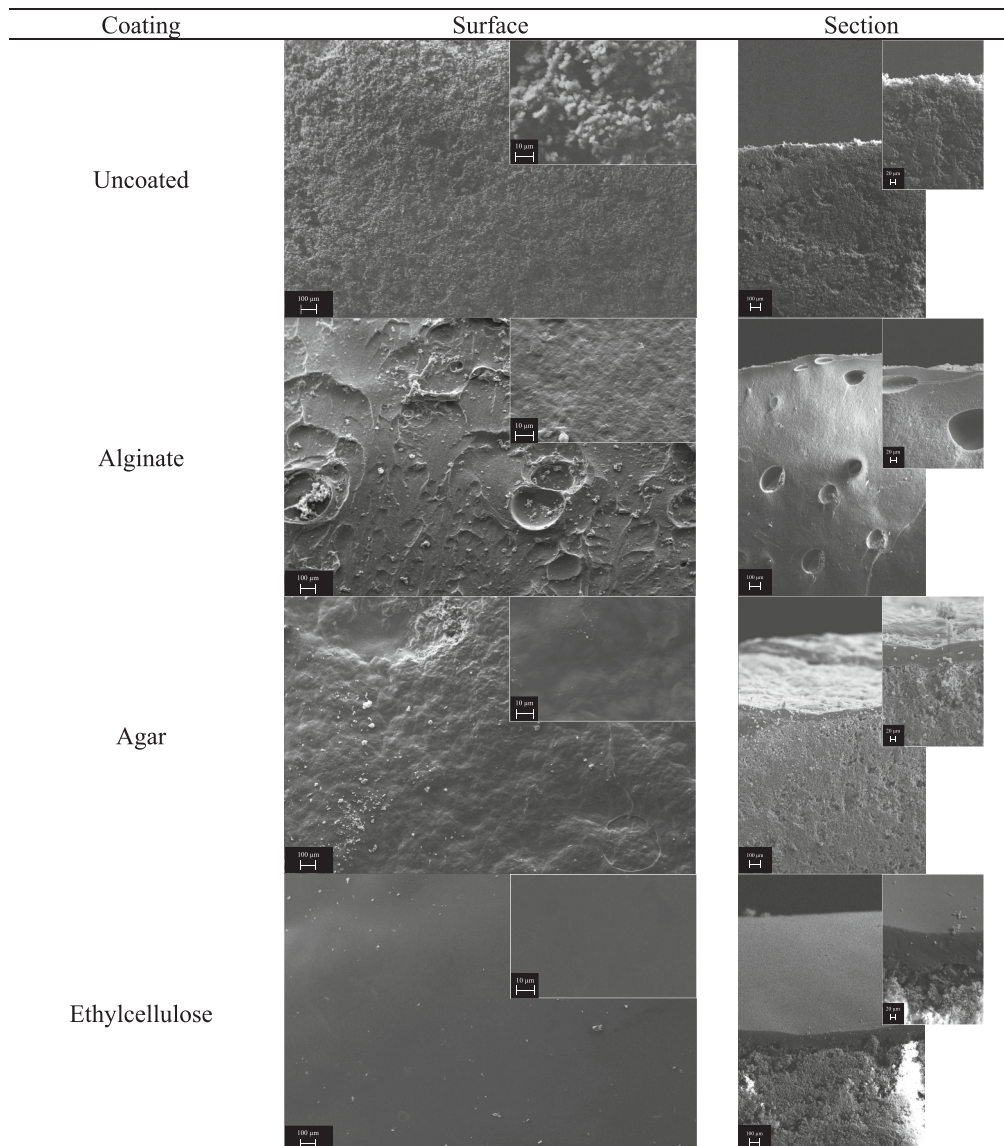


Fig. 1. SEM images of surface and section of aerogels coated with alginate, agar or ethylcellulose. Uncoated aerogel is also shown as control.

intense volume shrinkage observed upon aerogel dipping into the AL aqueous solution (Table 1). Upon AG coating, the typical microgel structure was no longer clearly appreciable at the aerogel surface, which appeared rough and uneven. Section micrographs evidenced the presence on the aerogel surface of a continuous coating layer of about 65 μm thickness. Below it, the microgel structure of the aerogel was still evident but characterized by coarser porosity as compared to the one of the control aerogel, confirming porosity data (Table 1). In fact, the original microgel spherical aggregates appeared partially fused together, possibly confirming the occurrence of minor structural collapse upon coating. The EC-coated aerogel showed the presence of a coating layer of approximately 100 μm thickness, characterized by an even and smooth surface. Section micrographs also demonstrated that the EC layer completely covered the surface of the aerogel, which presented a porous microgel structure analogous to that of the control, thus confirming the porosity results shown in Table 1. Based on this evidence, the higher firmness of the EC-coated aerogel (Table 1) could be directly attributed to the stiffness of the EC-coating layer. In order to confirm this hypothesis, EC coating was removed from the aerogel surface using a microtome blade to expose its bare surface. The firmness of the bare aerogel resulted comparable to that of the control sample,

demonstrating that the EC coating influenced the overall mechanical properties of the sample without affecting its internal structure (Antonyuk et al., 2015).

3.2. Moisture adsorption

To estimate the effect of coating on aerogel moisture adsorption, coated aerogels were maintained at relative humidity approaching 100% and the amount of adsorbed water vapour was measured (Fig. 2). The attention was focused on AG and EC-coated aerogels. By contrast, no further analyses were carried out on the AL-coated one, which showed intense structural collapse during coating application (Table 1 and Fig. 1).

All samples showed progressive adsorption of moisture (Fig. 2) with consequent swelling and firmness loss (Table 2). The extent of these changes was affected by the presence and the nature of the coating. In the first minutes of the moisture adsorption (inset Fig. 2), the AG-coated sample presented lower moisture adsorption than the uncoated one. However, extending the exposure of samples to moisture, a cross point was reached and the AG-coated aerogel showed a higher ability to interact with water vapour than the uncoated one. This result apparently

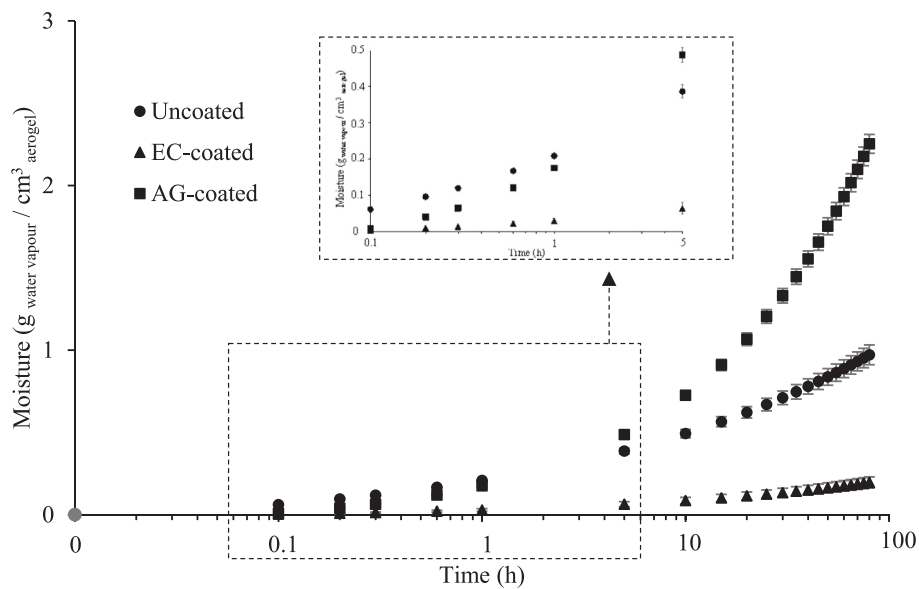


Fig. 2. Water vapour adsorption of uncoated aerogel and of aerogels coated with agar (AG) or ethylcellulose (EC) during maintenance at 100% ERH. The inset figure highlights water vapour adsorption in the first minutes.

Table 2

Volume change and firmness of uncoated aerogel and of aerogels coated with agar or ethylcellulose after 7 days of water vapour adsorption.

Coating	Volume variation (%) ^a	Firmness variation (%) ^a
Uncoated	+ 32.91 ± 0.24 ^a	-84.52 ± 0.03 ^a
Agar	+ 13.57 ± 0.56 ^b	-83.22 ± 0.01 ^b
Ethylcellulose	+ 5.70 ± 0.03 ^c	-67.61 ± 0.07 ^c

^{a, b, c}: means indicated by different letters in the same column are significantly different ($p < 0.05$).

^a Variation is expressed in relation to uncoated, AG-coated, and EC-coated aerogels prior to adsorption (Table 1).

contradicts the partial collapse of the AG-coated aerogel (Table 1), which would account for a lower capacity of water adsorption in the aerogel pores. Nevertheless, these results could be explained by the high hygroscopicity and hydrophilicity of AG (Arham et al., 2016; Phan et al., 2005). Probably, the uncoated aerogel initially had a greater ability to adsorb moisture due to its open porosity, contrary to the AG-coated

aerogel which presented a protective surface AG layer. Nevertheless, the latter would be able to progressively adsorb larger water amounts over a longer time scale (1–5 days). In addition, despite the higher amount of moisture adsorbed by the AG-coated aerogel as compared to the control one (Fig. 2), it showed a lower volume increase as compared to the uncoated one (Table 2). This result suggests that most of the water vapour was not adsorbed onto the internal pore surface of the AG-coated sample but rather within the hygroscopic AG coating layer.

As expected, the hydrophobic EC coating resulted in the lowest moisture adsorption (Fig. 2), which also accounted for a lower swelling and firmness loss as compared to the uncoated sample (Table 2) (Wu et al., 2018). EC coatings are indeed exploited in pharmaceutical applications, as physical barriers able to protect sensitive compounds from ambient humidity (Adeleke, 2019; Mehta et al., 2016; Romero-Bastida et al., 2004).

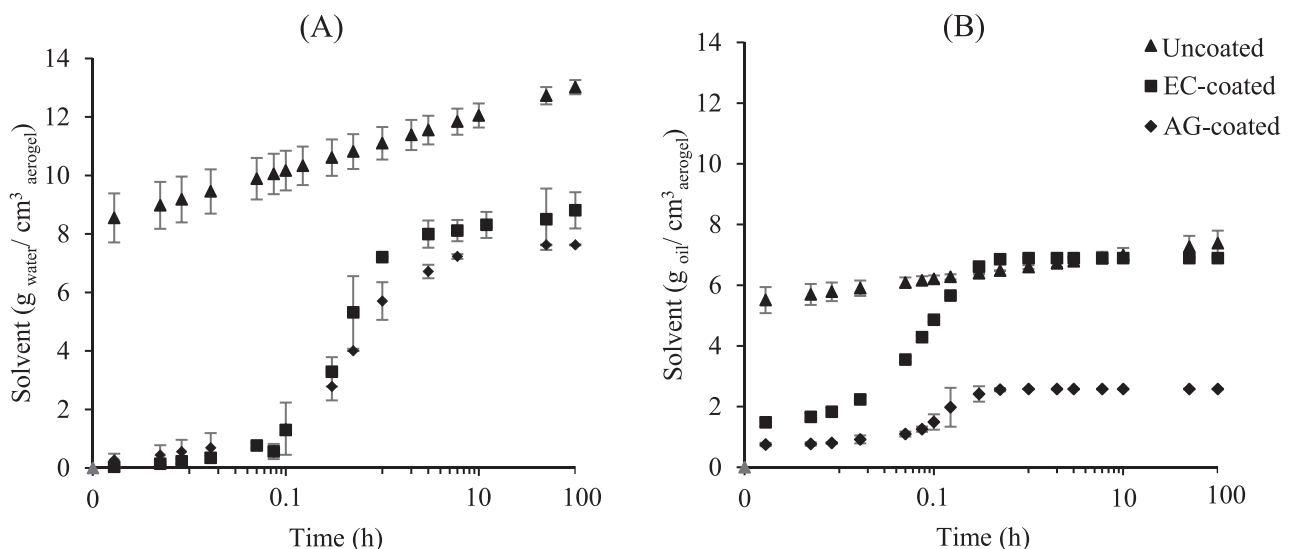


Fig. 3. Solvent absorption of uncoated aerogel and of aerogels coated with agar (AG) or ethylcellulose (EC) during immersion into water (A) or oil (B).

Table 3

Volume and firmness variation of uncoated aerogels and of aerogels coated with agar (AG) or ethylcellulose (EC) after 100 h water or oil absorption.

Coating	Water		Oil	
	Volume variation (%) ^a	Firmness variation (%)	Volume variation (%) ^a	Firmness variation (%) ^a
Uncoated	+27.54 ± 5.62 ^a	-92.51 ± 0.01 ^a	-19.06 ± 0.10 ^a	-0.07 ± 0.13 ^b
Agar	+9.45 ± 0.23 ^b	-89.61 ± 0.02 ^b	-0.55 ± 0.22 ^c	-30.07 ± 0.09 ^a
Ethylcellulose	+3.44 ± 0.33 ^c	-87.52 ± 0.01 ^c	-7.73 ± 0.05 ^b	-8.46 ± 0.13 ^c

^{a, b, c}: means indicated by different letters in the same column are significantly different ($p < 0.05$).

* Variation is expressed in relation to uncoated, AG-coated, and EC-coated aerogels prior to absorption (Table 1).

3.3. Water and oil uptake



To further study the capacity of coated aerogels to interact with common food solvents, water and oil absorption of uncoated and AG- and EC-coated samples was evaluated over time (Fig. 3).

The uncoated aerogels showed immediate water and oil absorption upon contact with both solvents, followed by a slower uptake, which did not level off even after 15 h. Water uptake in the uncoated aerogel (Fig. 3A) was higher than the oil one (Fig. 3B), probably due to the hydrophilicity of the WP aerogel network. Moreover, water uptake by the uncoated aerogel was associated with swelling and significant loss of firmness (Table 3). According to the literature, this is attributed to the progressive weakening of the interactions among WP backbones in favour of their interaction with water molecules (Manzocco et al., 2022). By contrast, lower variations in aerogel volume and firmness were observed upon oil absorption, possibly indicating that oil was simply absorbed into the aerogel pores with limited interactions with the WP network. Similar results were reported in previous works studying the absorption behavior of aerogels from hydrophilic biopolymers, including WP (Manzocco et al., 2022) and vegetable fibers (Plazzotta et al., 2018).

AG- and EC-coated aerogels presented a solvent absorption behavior considerably different than that observed for the uncoated sample (Fig. 3). An initial lag phase was detected in all cases, indicating the capacity of coating to delay solvent absorption in the aerogel structure. Nevertheless, after this initial lag phase, the solvents were progressively absorbed, reaching a plateau value. As regards the AG-coated aerogel, the overall water and oil uptake after 10 h was respectively about 40 and 60% lower than that observed for the uncoated sample. The lowest oil and water absorption of the AG-coated sample compared to the uncoated aerogel is probably due to the volume contraction upon AG coating (Table 1). Thanks to its lipophilic nature, the EC-coated aerogel was able to reduce water uptake, so that the plateau value was about 30% lower than that of the uncoated aerogel. Since this sample showed a volume analogous to that of the uncoated aerogel (Table 1), the lower overall water absorption cannot be attributed to a lower pore volume available for water uptake. Rather, the occurrence of a physical hindrance to progressive swelling and impregnation with water might be hypothesised. In other words, the firm and rigid EC coating layer (Table 1) might act as a cage entrapping the aerogel and preventing its swelling (Table 3). By contrast, EC-coating aerogel was not effective in reducing oil absorption, which reached values analogous to those of the uncoated aerogel within 100 h (Fig. 3B). This was probably due to the solubilization of the EC coating layer in the oil (Wasilewska & Winnicka, 2019).

Table 4

Appearance, volume, firmness and weight variation of uncoated aerogel and of aerogel coated with agar (AG) after immersion into a lipophilic food system, made of coconut stearin and sunflower oil.

Coating	Appearance	Volume variation (%) ^a	Firmness variation (%) ^a	Weight variation (%) ^a
Uncoated		-1.74 ± 0.81 ^a	-3.41 ± 0.06 ^b	+202.18 ± 1.65 ^a
Agar		-0.43 ± 0.09 ^a	-25.53 ± 0.05 ^a	+96.34 ± 1.68 ^b

^{a, b}: means indicated by different letters in the same column are significantly different ($p < 0.05$).

* Variation is expressed in relation to uncoated and AG-coated aerogels prior to absorption (Table 1).

3.4. Interaction of coated aerogels with water and oil in model food systems



Based on the ability of AG and EC coating layers to steer aerogel oil and water absorption, respectively, their performance with more complex food systems was evaluated. Specifically, the AG-coated aerogel was immersed in a lipophilic food system, made of a mixture of coconut stearin and sunflower oil. By contrast, the EC-coated aerogel was immersed in an aqueous food system, consisting of a batter made of water and flour.

Table 4 reports the appearance and the physical characteristics of the AG-coated aerogel compared to the uncoated one after contact for 5 h with the lipidic food system.

The uncoated aerogel showed a whitish appearance, slight shrinkage and firmness variation as well as a massive weight increase following the absorption of lipids. By contrast, the AG-coated aerogel presented a more yellow colour, probably due to the yellowish colour of the AG-coated aerogel (Table 1), and much lower oil absorption, as indicated by the lower weight increase (Table 4). In any case, the firmness variations of the uncoated and AG-coated aerogels upon contact with the lipidic food system (Table 4) were similar to those observed upon oil

Table 5

Appearance, volume, firmness and weight variation of uncoated aerogel and of aerogel coated with ethylcellulose (EC) after immersion into a hydrophilic food system made of flour and water.

Coating	Appearance	Volume variation (%) ^a	Firmness variation (%) ^a	Weight variation (%) ^a
Uncoated		+19.42 ± 0.65 ^a	-83.29 ± 0.01 ^b	+217.76 ± 10.07 ^a
Ethylcellulose		+3.68 ± 0.20 ^b	-59.44 ± 0.05 ^a	+21.69 ± 1.23 ^b

^{a, b}: means indicated by different letters in the same column are significantly different ($p < 0.05$).

* Variation is expressed in relation to uncoated and EC-coated aerogels prior to absorption (Table 1).

absorption (Table 3). This indicates that the assessment of oil uptake into the aerogels (Table 3) actually accounts for their ability to absorb oil even in more complex systems.

Table 5 reports the appearance and the physical characteristics after immersion in the aqueous food system of the EC-coated sample as compared to the uncoated one.

The EC coating application was demonstrated to efficaciously reduce the absorption of the aqueous food system. In fact, after 5 h of immersion in the batter, the EC-coated aerogel structure was almost intact. By contrast, the uncoated aerogel partially disintegrated, showing an evident loss of the original shape and morphology. This result was confirmed by the significantly higher increase in sample volume and weight, and the higher firmness reduction of the uncoated sample as compared to the EC-coated aerogel.

4. Conclusions

In this work, monolithic WP aerogels were efficaciously coated by simple dipping in aqueous or alcoholic solutions containing food-grade polymers. Results highlighted rapid coating setting to be crucial in preserving the inner aerogel porous structure. The difference in coating polarity affected aerogel ability to interact with food systems characterized by different compositions and increasing complexity. A hydrophilic coating, although requiring specific protection from environmental moisture, might be used to efficaciously delay and reduce oil uptake. The ability of coating to protect the inner aerogel porous structure from oil uptake could open the possibility of developing aerated lipidic products, characterized by a reduced caloric density. By contrast, the application of a lipophilic coating to aerogels could allow reducing their moisture adsorption and water absorption. This strategy could be selected when aerogels loaded with bioactive molecules are intended as ingredients of aqueous foods to protect the loaded molecule during both storage and digestion. Moreover, steering the interaction of aerogels with digestive fluids could account for the controlled release of loaded bioactive molecules. Further functional advantages might be envisaged by combining different coating polymers within a mixed-composition coating layer or multiple coating layers.

Despite these interesting scenarios, the performance of coated aerogels during food formulation, process, storage and digestion is still unknown and worthy of further investigation. Finally, it is important to study the conditions allowing the translation of these findings from monolithic aerogels to particles, which are more likely to be included in complex food formulations. In this regard, the development of processes and equipment for the coating of small porous particles is far from trivial, requiring a meticulous setting of coating formulation and operative conditions to obtain a homogeneous and continuous coating layer positioned exclusively onto the particle surface.

CRedit authorship contribution statement

Lorenzo De Berardinis: Data curation, Formal analysis, Investigation, Methodology, Visualization, Writing – original draft, Writing – review & editing. **Stella Plazzotta:** Conceptualization, Methodology, Visualization, Writing – review & editing. **Michele Magnan:** Formal analysis, Writing – review & editing. **Lara Manzocco:** Conceptualization, Project administration, Resources, Supervision, Writing – review & editing.

Declaration of Competing Interest

None.

Data availability

Data will be made available on request.

Acknowledgements

This publication is based upon work from COST Action “Advanced Engineering of aeroGels for Environment and Life Sciences” (AEROGELS, ref. CA18125), supported by COST (European Cooperation in Science and Technology).

The authors thank Mrs. Diletta Marchesino for helping with sample preparation and analysis.

References

- Adeleke, O. A. (2019). Premium ethylcellulose polymer based architectures at work in drug delivery. *International Journal of Pharmaceutics*, 1, Article 100023. <https://doi.org/10.1016/J.IJPX.2019.100023>
- Alnaief, M., Antonyuk, S., Hentzschel, C. M., Leopold, C. S., Heinrich, S., & Smirnova, I. (2012). A novel process for coating of silica aerogel microspheres for controlled drug release applications. *Microporous and Mesoporous Materials*, 160, 167–173. <https://doi.org/10.1016/J.MICROMESO.2012.02.009>
- Antonyuk, S., Heinrich, S., Gurikov, P., Raman, S., & Smirnova, I. (2015). Influence of coating and wetting on the mechanical behaviour of highly porous cylindrical aerogel particles. *Powder Technology*, 285, 34–43. <https://doi.org/10.1016/J.POWTEC.2015.05.004>
- Arham, R., Mulyati, M. T., Metusalach, M., & Salengke, S. (2016). Physical and mechanical properties of agar based edible film with glycerol plasticizer. *International Food Research Journal*, 23, 1669–1675.
- Betz, M., García-González, C. A., Subrahmanyam, R. P., Smirnova, I., & Kulozik, U. (2012). Preparation of novel whey protein-based aerogels as drug carriers for life science applications. *The Journal of Supercritical Fluids*, 72, 111–119. <https://doi.org/10.1016/J.SUPFLU.2012.08.019>
- Chiu, N., Hewson, L., Yang, N., Linforth, R., & Fisk, I. (2015). Controlling salt and aroma perception through the inclusion of air fillers. *LWT - Food Science and Technology*, 63, 65–70. <https://doi.org/10.1016/J.LWT.2015.03.098>
- Ciuffarin, F., Négrier, M., Plazzotta, S., Libralato, M., Calligaris, S., Budtova, T., & Manzocco, L. (2023). Interactions of cellulose cryogels and aerogels with water and oil: Structure-function relationships. *Food Hydrocolloids*, 140, Article 108631. <https://doi.org/10.1016/j.foodhyd.2019.05.008>
- De Marco, I., & Reverchon, E. (2017). Starch aerogel loaded with poorly water-soluble vitamins through supercritical CO₂ adsorption. *Chemical Engineering Research and Design*, 119, 221–230. <https://doi.org/10.1016/J.CHERD.2017.01.024>
- Fernandes, L., Casal, S., Pereira, J. A., Pereira, E. L., Saraiva, J. A., & Ramalhosa, E. (2018). Effect of alginate coating on the physico-chemical and microbial quality of pansies (*Viola × wittrockiana*) during storage. *Food Science and Biotechnology*, 27, 987–996.
- Fischer, H., Polikarpov, I., & Craievich, A. F. (2004). Average protein density is a molecular-weight-dependent function. *Protein Science*, 13, 2825–2828. <https://doi.org/10.1110/ps.04688204>
- Fricke, J., & Tillotson, T. (1997). Aerogels: Production, characterization, and applications. *Thin Solid Films*, 297, 212–223. [https://doi.org/10.1016/S0040-6090\(96\)09441-2](https://doi.org/10.1016/S0040-6090(96)09441-2)
- García-González, C. A., Budtova, T., Durães, L., Del Gaudio, P., Gurikov, P., Koebel, M., ... Smirnova, I. (2019). An opinion paper on aerogels for biomedical and environmental applications. *Molecules*, 24, 1815. <https://doi.org/10.3390/molecules24091815>
- García-González, C. A., Jin, M., Gerth, J., Alvarez-Lorenzo, C., & Smirnova, I. (2015). Polysaccharide-based aerogel microspheres for oral drug delivery. *Carbohydrate Polymers*, 117, 797–806. <https://doi.org/10.1016/J.CARBPOL.2014.10.045>
- García-González, C. A., & Smirnova, I. (2013). Use of supercritical fluid technology for the production of tailor-made aerogel particles for delivery systems. *Journal of Supercritical Fluids*, 79, 152–158. <https://doi.org/10.1016/j.supflu.2013.03.001>
- Goslinska, M., Selmer, I., Kleemann, C., Kulozik, U., Smirnova, I., & Heinrich, S. (2019). Novel technique for measurement of coating layer thickness of fine and porous particles using focused ion beam. *Particology*, 42, 190–198. <https://doi.org/10.1016/J.PARTIC.2018.03.002>
- Hjartstam, J., & Hjertberg, T. (1999). Studies of the water permeability and mechanical properties of a film made of an ethyl cellulose-ethanol-water ternary mixture. *Journal of Applied Polymer Science*, 74, 2056–2062. [https://doi.org/10.1002/\(SICI\)1097-4628\(19991121\)74:8<2056::AID-APP21>3.0.CO;2-Y](https://doi.org/10.1002/(SICI)1097-4628(19991121)74:8<2056::AID-APP21>3.0.CO;2-Y)
- Jung, I., Schroeter, B., Plazzotta, S., De Berardinis, L., Smirnova, I., Gurikov, P., & Manzocco, L. (2023). Oleogels from mesoporous whey and potato protein based aerogel microparticles: Influence of microstructural properties on oleogelation ability. *Food Hydrocolloids*, 142, Article 108758. <https://doi.org/10.1016/J.FOODHYD.2023.108758>
- Kim, S., Lee, H., Kim, D., Ha, H., Qaiser, N., Yi, H., & Hwang, B. (2020). Ethylcellulose/agar nanowire composites as multifunctional patchable transparent electrodes. *Surface and Coatings Technology*, 394, Article 125898. <https://doi.org/10.1016/J.SURFCOAT.2020.125898>
- Kleemann, C., Schuster, R., Rosenecker, E., Selmer, I., Smirnova, I., & Kulozik, U. (2020). In-vitro-digestion and swelling kinetics of whey protein, egg white protein and sodium caseinate aerogels. *Food Hydrocolloids*, 101, Article 105534. <https://doi.org/10.1016/J.FOODHYD.2019.105534>
- Mallepally, R. R., Bernard, I., Marin, M. A., Ward, K. R., & McHugh, M. A. (2013). Superabsorbent alginate aerogels. *Journal of Supercritical Fluids*, 79, 202–208. <https://doi.org/10.1016/J.SUPFLU.2012.11.024>

- Manzocco, L., Mikkonen, K. S., & García-González, C. A. (2021). Aerogels as porous structures for food applications: Smart ingredients and novel packaging materials. *Food Structure*, 28, Article 100188. <https://doi.org/10.1016/j.foostr.2021.100188>
- Manzocco, L., Plazzotta, S., Powell, J., de Vries, A., Rousseau, D., & Calligaris, S. (2022). Structural characterisation and sorption capability of whey protein aerogels obtained by freeze-drying or supercritical drying. *Food Hydrocolloids*, 122, Article 107117. <https://doi.org/10.1016/j.foodhyd.2021.107117>
- Manzocco, L., Valoppi, F., Calligaris, S., Andreatta, F., Spilimbergo, S., & Nicoli, M. C. (2017). Exploitation of κ-carrageenan aerogels as template for edible oleogel preparation. *Food Hydrocolloids*, 71, 68–75. <https://doi.org/10.1016/j.foodhyd.2017.04.021>
- Mehta, R., Teckoe, J., Schoener, C., Workentine, S., Ferrizzi, D., & Rajabi-Siahboomi, A. (2016). Investigation into the effect of ethylcellulose viscosity variation on the drug release of metoprolol tartrate and acetaminophen extended release multiparticulates—Part I. *AAPS PharmSciTech*, 17, 1366–1375. <https://doi.org/10.1208/S12249-015-0465-Z/FIGURES/9>
- Naftaly, M., Tikhomirov, I., Hou, P., & Markl, D. (2020). Measuring open porosity of porous materials using THz-TDS and an index-matching medium. *Sensors*, 20, 3120. <https://doi.org/10.3390/s20113120>
- Osterholt, K. M., Roe, L. S., & Rolls, B. J. (2007). Incorporation of air into a snack food reduces energy intake. *Appetite*, 48, 351–358. <https://doi.org/10.1016/j.appet.2006.10.007>
- Parreidt, T. S., Müller, K., & Schmid, M. (2018). Alginate-based edible films and coatings for food packaging applications. *Foods*, 7, 170. <https://doi.org/10.3390/foods7100170>
- Phan, T. D., Debeaufort, F., Luu, D., & Voilley, A. (2005). Functional properties of edible agar-based and starch-based films for food quality preservation. *Journal of Agricultural and Food Chemistry*, 53, 973–981. <https://doi.org/10.1021/JF040309S/ASSET/IMAGES/LARGE/JF040309SF00006.JPEG>
- Plazzotta, S., Alongi, M., De Berardinis, L., Melchior, S., Calligaris, S., & Manzocco, L. (2022). Steering protein and lipid digestibility by oleogelation with protein aerogels. *Food & Function*, 13, 10601–10609. <https://doi.org/10.1039/D2FO01257J>
- Plazzotta, S., Calligaris, S., & Manzocco, L. (2018). Innovative bioaerogel-like materials from fresh-cut salad waste via supercritical-CO₂-drying. *Innovative Food Science and Emerging Technologies*, 47, 485–492. <https://doi.org/10.1016/j.ifset.2018.04.022>
- Plazzotta, S., Calligaris, S., & Manzocco, L. (2020). Structural characterization of oleogels from whey protein aerogel particles. *Food Research International*, 132, Article 109099. <https://doi.org/10.1016/j.foodres.2020.109099>
- Plazzotta, S., Jung, I., Schroeter, B., Subrahmanyam, R. P., Smirnova, I., Calligaris, S., ... Manzocco, L. (2021). Conversion of whey protein aerogel particles into oleogels: Effect of oil type on structural features. *Polymers*, 13, 4063. <https://doi.org/10.3390/POLYM13234063/S1>
- Romero-Bastida, C. A., Flores-Huicochea, E., Martin-Polo, M. O., Velazquez, G., & Torres, J. A. (2004). Compositional and moisture content effects on the biodegradability of zein/ethylcellulose films. *Journal of Agricultural and Food Chemistry*, 52, 2230–2235. <https://doi.org/10.1021/jf0350414>
- dos Santos, P., Viganó, J., de Furtado, G. F., Cunha, R. L., Hubinger, M. D., Rezende, C. A., & Martínez, J. (2020). Production of resveratrol loaded alginate aerogel: Characterization, mathematical modeling, and study of impregnation. *Journal of Supercritical Fluids*, 163, Article 104882. <https://doi.org/10.1016/j.supflu.2020.104882>
- Schroeter, B., Yonkova, V. P., Goslinska, M., Orth, M., Pietsch, S., Gurikov, P., ... Heinrich, S. (2021). Spray coating of cellulose aerogel particles in a miniaturized spouted bed. *Cellulose*, 28, 7795–7812. <https://doi.org/10.1007/S10570-021-04032-0/TABLES/5>
- Selmer, I., Kleemann, C., Kulozik, U., Heinrich, S., & Smirnova, I. (2015). Development of egg white protein aerogels as new matrix material for microencapsulation in food. *The Journal of Supercritical Fluids*, 106, 42–49. <https://doi.org/10.1016/j.supflu.2015.05.023>
- Sousa, A. M. M., Sereno, A. M., Hilliou, L., & Gonçalves, M. P. (2010). Biodegradable agar extracted from gracilaria vermiculophylla: Film properties and application to edible coating. *Materials Science Forum*, 636, 739–744. <https://doi.org/10.4028/WWW.SCIENTIFIC.NET/MSF.636-637.739>
- Ubeyitogullari, A., Moreau, R., Rose, D. J., & Ciftci, O. N. (2019). In vitro bioaccessibility of low-crystallinity phytosterol nanoparticles generated using nanoporous starch bioaerogels. *Journal of Food Science*, 84, 1812–1819. <https://doi.org/10.1111/1750-3841.14673>
- Wasilewska, K., & Winnicka, K. (2019). Ethylcellulose—A pharmaceutical excipient with multidirectional application in drug dosage forms development. *Materials*, 12, 3386. <https://doi.org/10.3390/MA12203386>
- Wu, K., Zhu, Q., Qian, H., Xiao, M., Corke, H., Nishinari, K., & Jiang, F. (2018). Controllable hydrophilicity-hydrophobicity and related properties of konjac glucomannan and ethyl cellulose composite films. *Food Hydrocolloids*, 79, 301–309. <https://doi.org/10.1016/j.foodhyd.2017.12.034>